Bioorganic Chemistry xxx (xxxx) xxxx

Contents lists available at ScienceDirect

Bioorganic Chemistry

journal homepage: www.elsevier.com/locate/bioorg

Amphiphilic azobenzenes: Antibacterial activities and biophysical investigation of their interaction with bacterial membrane lipids

A. Franche[a], A. Fayeulle[a], L. Lins[b], M. Billamboz[c], I. Pezron[a], M. Deleu[b,*], E. Léonard[d,*]

[a] Sorbonne University, Université de technologie de Compiègne, ESCOM, EA TIMR 4297, Centre de recherche de Royallieu, CS 60319, 60203 Compiègne Cedex, France
[b] TERRA Research Center, Laboratory of Molecular Biophysics at Interfaces, SFR Condorcet, Gembloux Agro-Bio Tech, University of Liege, Passage des Déportés, 2, 5030 Gembloux, Belgium
[c] Laboratoire de chimie durable et santé, Yncrea Hauts-de-France, HEI, 13 rue de Toul, 59046 Lille Cedex, France
[d] ESCOM, UTC, EA TIMR 4297, 1 allée du Réseau Jean-Marie Buckmaster, 60200 Compiègne, France

ARTICLE INFO

Keywords:
Azo amphiphile compounds
Organic synthesis
Antibacterial activity
Membrane interaction

ABSTRACT

With the emergence of multi-drug resistant bacteria and hospital-acquired infections, there is an urgent need to develop new antibiotics. Here, we report the synthesis, physico-chemical characterizations, and antimicrobial activity assays of four Azo compounds that differ in their alkyl chain length. The molecular mechanism of their antibacterial activity was investigated by complementary *in vitro* and *in silico* biophysical studies. The compounds with alkyl chain lengths of four or six carbons showed a low MIC_{50} against *Escherichia coli* and *Bacillus subtilis*. Our investigations into the mechanism of their action revealed that phosphatidylethanolamine in the bacterial plasma membrane plays an important role in their antibacterial activity.

1. Introduction

The emergence of nosocomial multi-drug resistant (MDR) bacterial strains is a growing concern in hospitals and underlines the urgent need for the development of novel antibacterial agents [1,2]. The azo compounds are used in a wide range of applications such as surfactants [3–5], catalysts [6], gelators [7], and liquid crystals [8,9]. Recently, azo-amphiphiles have been shown to exhibit a high biocide potential, especially if they contain a cationic head group such as quaternary ammonium salt. Although azobenzene derived compounds can exist either as *cis* or *trans* isomer, in the case of the quaternary ammonium derivative azobenzene derivative, the *trans*-isomer displayed more potent antimicrobial activity than the *cis*-isomer [10]. Azo compounds are well known to interact with the bacterial cell membrane [11–13] and the membrane permeabilizing effect of the quaternary ammonium *trans* derivatives was shown to be greater than the *cis* one [10]. However, the molecular details of the mechanism are not well documented. In this context, our strategy was to synthesize novel amphiphilic bioactive azobenzenes, to evaluate their potential as antibacterial agents and to investigate their interaction with model membranes that mimic the plasma membrane of bacteria, to elucidate the mechanism of their antibacterial activities.

Two rod-shaped bacteria, *Escherichia coli* and *Bacillus subtilis*, were considered for antibacterial tests because of their different cell wall structures (*E. coli* as a gram-negative model and *B. subtilis* as gram-positive) and because they belong to species encompassing pathogenic MDR strains [14,15].

2. Results and discussion

2.1. Synthesis

Starting from 4-alkyl-azobenzene-4′-alcohols (**1a–1d**) [4,16–18], we performed Williamson reaction with 2-chloroethanol in the presence of potassium iodide and potassium carbonate to get azobenzenes (**2a–2d**) with yields of 34–79%. Tosylation of the primary alcohol gave derivatives **3a–3d**, but the products were found to be highly unstable. Therefore, they were used in the next step without purification to prevent any degradation during the purification steps. Finally, nucleophilic substitution followed by amine quaternarization led to the target products, *trans*-H-AZOTAI **4a**, *trans*-Et-AZOTAI **4b**, *trans*-Bu-AZOTAI **4c**, and *trans*-Hex-AZOTAI **4d** with yields of 10% to 98% (see Scheme 1).

The overall yields of the products were 8% (*trans*-H-AZOTAI **4a**, R = H), 16% (*trans*-Et-AZOTAI **4b**, R = C_2H_5), 33% (*trans*-Bu-AZOTAI **4c**, R = C_4H_9), and 10% (*trans*-Hex-AZOTAI **4d**, R = C_6H_{13}). The yield of product **4c** was higher than other compounds because of ease of purification.

* Corresponding authors.
E-mail addresses: magali.deleu@uliege.be (M. Deleu), e.leonard@escom.fr (E. Léonard).

https://doi.org/10.1016/j.bioorg.2019.103399
Received 9 August 2019; Received in revised form 23 October 2019; Accepted 24 October 2019

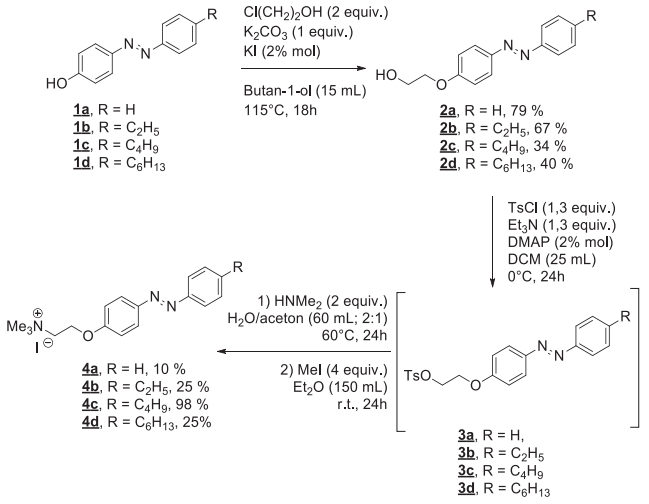

Scheme 1. Synthesis of AZOTAI family.

2.2. Properties in solution

The amphiphilic property of all native *trans* isomers **4a–4d** was studied by monitoring the decrease in the equilibrium surface tension of water with increasing concentrations of the compound. The *trans*-isomer composition in the compounds were 76%, *trans*-H-AZOTAI **4a**; 88%, *trans*-Et-AZOTAI **4b**; 90%, *trans*-Bu-AZOTAI **4c**; and 80%, *trans*-Hex-AZOTAI **4d**. As shown in Fig. 1, when the equilibrium surface tension was plotted against the concentration for **4a–4d** compounds characteristic break points were observed suggesting that these compounds were able to form micelles in water.

Table 1 gives the critical micellar concentration (CMC) values and the corresponding surface tension for each compound.

As it was commonly observed with surface-active molecules [19] including alkyl derivatives of quaternary ammonium compounds [20,21], an increase in the length of the nonpolar alkyl chain reduces the value of the CMC. The γ_{CMC} observed for the **4b–4d** compounds are similar and much lower than that observed for **4a**. Thus, the adsorption of **4b–4d** compounds at the air-water interface was found to be energetically favourable. This suggested that their adsorption onto a hydrophilic/hydrophobic interface like a bacterial membrane would also be energetically favourable.

2.3. Antibacterial activities

We tested the compounds **4a–4d** for their capacity to inhibit the bacterial growth on two model bacteria, *E. coli* and *B. subtilis*. Polymyxin B, a commercial antibacterial compound used to target gram-negative outer membrane [22] was used as positive control to evaluate the activity of **4a–4d** against the gram-negative model *E. coli*. Daptomycin, a commercial antibacterial compound that dissipates the cytoplasmic membrane potential of gram-positive bacteria [23] was used as positive control to evaluate the activity of compounds **4a–4d** against *B. subtilis*.

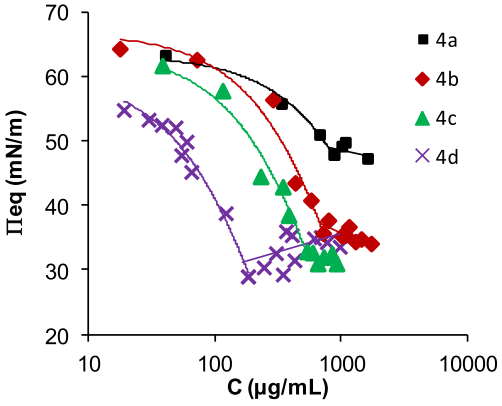

Fig. 1. Change in the equilibrium surface tension (IIeq) as a function of the concentration (C) of **4a–4d** in water. **4a**: *trans*-H-AZOTAI; **4b**: *trans*-Et-AZOTAI; **4c**: *trans*-Bu-AZOTAI; **4d**: *trans*-Hex-AZOTAI.

Table 1
Critical Micelle Concentration (CMC) values in µg/mL and surface tension at the CMC (γ_{CMC}) in mN/m.

	Trans-H-AZOTAI **4a**	*Trans*-Et-AZOTAI **4b**	*Trans*-Bu-AZOTAI **4c**	*Trans*-Hex-AZOTAI **4d**
CMC (µg/mL)	746 ± 4	682 ± 7	563 ± 5	171 ± 4
γ_{CMC} (mN/m)	49.2 ± 4.6	36.7 ± 6.9	32.4 ± 5.1	31.1 ± 4.1

Table 2
Values in µg/mL of the minimum inhibitory concentration triggering at least 50% of growth inhibition (MIC_{50}) and of minimum inhibitory concentration (MIC) for the azobenzene compounds, daptomycin and polymyxin B against *E. coli* and *B. subtilis*.

MIC_{50}	Daptomycin	Polymyxin B	**4a**	**4b**	**4c**	**4d**
E. coli	–	3.75	> 30	> 30	> 30	7.5
B. subtilis	30	–	> 30	7.5	2	2
MIC	Daptomycin	Polymyxin B	4a	4b	4c	4d
E. coli	–	< 1	> 30	3.75	7.5	2
B. subtilis	15	–	> 30	7.5	2	2

Table 2 shows minimum inhibitory concentration (MIC) and MIC_{50}, the concentration at which 50% of growth inhibition occurred, for the four compounds **4a–4d** and the controls.

Compound *trans*-H-AZOTAI **4a** triggered no inhibition of the two bacteria within the concentration range tested. However, *trans*-Et-AZOTAI **4b** and *trans*-Bu-AZOTAI **4c** showed low MIC_{50} towards *B. subtilis* but no activity against *E. coli*. On the other hand, *trans*-Hex-AZOTAI **4d** showed a very low MIC_{50} against both *E. coli* and *B. subtilis*. In the literature, other quaternary ammonium compounds have shown a high MIC_{50} towards *E. coli*. For example, the MIC_{50} of didecyldimethylammonium chloride is 16 µg/mL and the MIC_{50} of cetyltrimethylammonium bromide is 256 µg/mL [24]. Thus, in comparison to these other quaternary ammonium compounds, our compounds, *trans*-Et-AZOTAI **4b**, *trans*-Bu-AZOTAI **4c**, and, in particular, *trans*-Hex-AZOTAI **4d** appear to display comparatively low MIC_{50} towards *E. coli*. This result is promising even though MIC results from different studies must be compared with caution due to variations in susceptibility between strains. Moreover against the spores of *B. subtilis*, chlorhexidine digluconate, a quaternary ammonium compound, has been shown to have a MIC_{50} of 1 µg/mL [25], which is in the same concentration range as *trans*-Bu-AZOTAI **4c** and *trans*-Hex-AZOTAI **4d** in our work.

It is evident from our results that an increase in the nonpolar alkyl chain length enhances the biological activities of the Azo compounds, in accordance with other studies on mannosylerythritol [26] or aminoacridine [24]. The compounds **4b–4d** showed better antibacterial activity than the positive control daptomycin against *B. subtilis*. However, compared to polymyxin B, the antibacterial activity of *trans*-Bu-AZOTAI **4c** and *trans*-Hex-AZOTAI **4d** was lower against *E. coli*. This could be explained by the different mechanisms of action of the drugs. It is known that polymyxin B acts on the outer membrane of gram negative bacteria [22] by binding to the lipopolysaccharide, which explains its higher activity on this type of bacteria. For the azobenzene derivatives, we hypothesize that they act on the inner plasma membrane rather than on the outer plasma membrane. In particular, results obtained for the

compound *trans*-Hex-AZOTAI **4d** seemed to be interesting. Admittedly, the obtained MIC and MIC_{50} values for the latter compound was slightly higher than those of polymyxin B for *E. coli*, but the compound *trans*-Hex-AZOTAI **4d** also displayed a significant activity against *B. subtilis,* even better than daptomycin. Thus, this compound could have the advantage of a broad spectrum antimicrobial activity compared to the positive controls.

2.4. Biophysical investigation of the mechanism

As they showed the best antibacterial activities among the synthesized compounds, the mechanism of only *trans*-Bu-AZOTAI **4c** and *trans*-Hex-AZOTAI **4d** was investigated.

The IMPALA procedure [27] was applied to predict the capacity of insertion of *trans*-Bu-AZOTAI **4c** and *trans*-Hex-AZOTAI **4d** into an implicit model membrane. Briefly, the implicit membrane is described as a continuous medium where the properties vary only along the z-axis perpendicular to the bilayer plane. The membrane properties are represented by energy restraints (Epho and Elip, see Experimental section). The *trans*-Bu-AZOTAI **4c** or *trans*-Hex-AZOTAI **4d** molecule was systematically moved along the z axis from one side of the membrane to the other and the total restraint (Epho + Elip) was calculated for each position. A profile of the energy restraints as a function of the mass centre penetration into the implicit bilayer was then obtained (Fig. 2). For both molecules, the total restraint energy was much higher outside the bilayer than inside, suggesting that the insertion of both molecules within the membrane was energetically favourable. No sharp minimum was observed between −18 and 18 Å indicating that the molecules are probably able to move within the bilayer.

Experimentally, we analysed the permeabilizing effect of azobenzene compounds on experimental membrane models. Large unilamellar vesicles (LUVs) were formed with a lipid composition mimicking the plasma membrane of the two bacteria, *E. coli* and *B. subtilis* [28,29]. The permeabilization of the model membranes was quantified by measuring the increase in the fluorescence emission of calcein, resulting from the azo-compound induced release of the dye from the internal compartment of the vesicle, where it exists in a self-quenched state, into the external environment following interaction between the Azo compounds and the membrane.

As shown in Fig. 3, *trans*-Hex-AZOTAI **4d** has a significantly higher permeabilizing effect than *trans*-Bu-AZOTAI **4c**. Thus, longer chain length increased the destabilizing effect of the azobenzene derivatives,

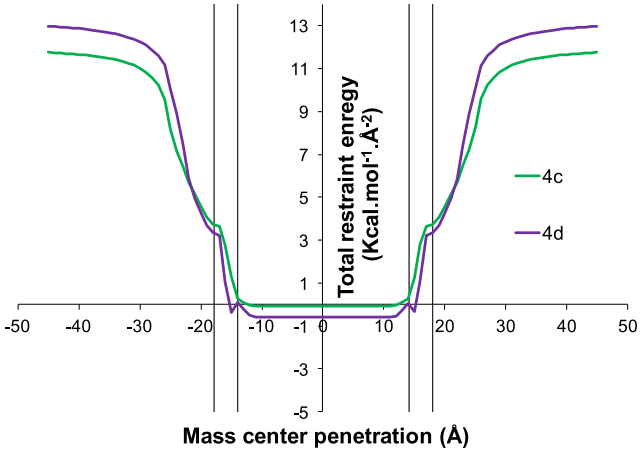

Fig. 2. Change in the total restraint energy as a function of the molecule mass centre penetration in an implicit bilayer obtained by IMPALA procedure. The vertical lines correspond (from left to right) to the interface between the bilayer and the aqueous phase (z = 18 Å), the interface between the hydrocarbon core and the lipid hydrophilic head (z = 13.5 Å), and the centre of the bilayer (z = 0 Å). **4c**: *trans*-Bu-AZOTAI; **4d**: *trans*-Hex-AZOTAI.

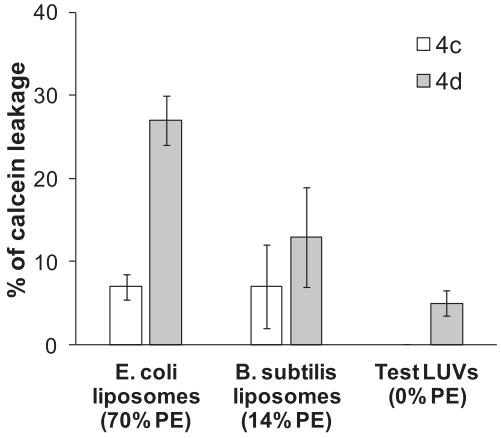

Fig. 3. Calcein leakage from LUVs containing phosphatidylethanolamine (PE) and mimicking *E. coli* (*E. coli*-like) or *B. subtilis*, (*B. subtilis*-like) or lacking PE (Test-LUVs) in the presence of Azo compounds, **4c** (*trans*-Bu-AZOTAI) or **4d** (*trans*-Hex-AZOTAI). The $C_{azobenzene}/C_{lipids}$ ratio was 0.25. The ordinate shows the amount of calcein released after 15 min in the presence of the azobenzene derivative as a percentage of the total amount released by Triton X-100. At least two independent experiments were performed. The percentage of calcein leakage from Test-LUVs in the presence of **4c** was zero.

which can be correlated with the CMC values (Table 1) and the antibacterial activity (Table 2). Nevertheless, a total release of calcein was not observed even at higher *trans*-Hex-AZOTAI **4d** concentrations suggesting that the mechanism of destabilization is related to a gradual release of the dye by all the vesicles following the annealing process that prevents further leakage [30] as already observed with D-xylose-based bolaamphiphiles [31].

Another important observation was the dependence between the calcein leakage and the percentage of phosphatidylethanolamine (PE) in the lipid composition of LUVs, from 70% to 0% PE. A higher PE content leads to an increase in the extent of permeabilization. This observation suggested that azobenzene derivatives have a specific interaction with PE.

To further analyse the specific interaction between the molecules *trans*-Bu-AZOTAI **4c** or *trans*-Hex-AZOTAI **4d** and the individual lipids composing the model membranes, adsorption experiments into a pure lipid monolayer composed of phosphatidylethanolamine (PE), phosphatidylglycerol (PG) or cardiolipin (CL) were performed using the Langmuir monolayer technique.

The adsorption was monitored by the increase of the surface pressure at a constant trough area for different initial surface pressures of the lipid monolayer in order to plot the maximal surface pressure variation (ΔΠ) versus the initial surface pressure (Πi) (see an example with PE monolayer in supplementary information).

From these curves, two different parameters can be determined (Fig. 4): the maximal insertion pressure (MIP) which reflects the penetration power of the molecule into a lipid monolayer, and the differential Π_0 ($d\Pi_0$) which indicates the (non-)attracting effect of the lipid towards the molecule.

All the MIP values were higher than 30–35 mN/m, the lateral pressure within biological membranes [32], suggesting that both azobenzene derivatives can insert into natural plasma membranes. The positive values of $d\Pi_0$ values confirm the affinity of the azobenzene derivatives for the individual lipid monolayers. This effect was higher for **4d** than **4c**, and in the case of **4d** the affinity was significantly higher towards PE monolayer than PG or CL monolayer.

Data from Langmuir monolayer experiments and calcein leakage assay strongly suggest that PE plays a key role in the interaction between azobenzene, and the membranes, especially for **4d**.

In parallel to the experimental approach, an *in silico* approach called Hypermatrix was used to study the lipid specificity and to obtain an

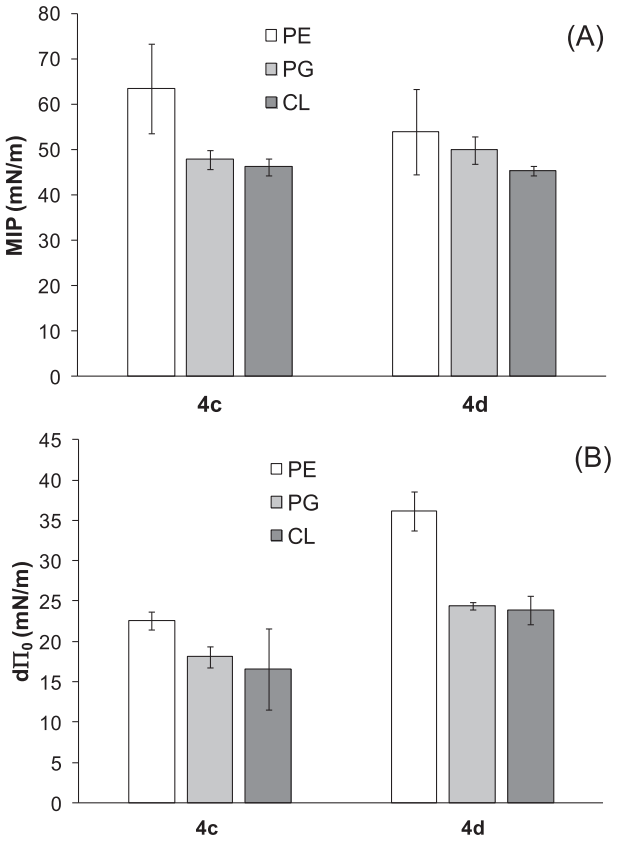

Fig. 4. Adsorption of azobenzene derivatives **4c** (*trans*-Bu-AZOTAI) or **4d** (*trans*-Hex-AZOTAI) into lipid monolayers: PE: phosphatidylethanolamine, PG: phosphatidylglycerol, CL: cardiolipin. (A) Maximal insertion pressure (MIP) and (B) differential Π_0 ($d\Pi_0$) values. These parameters are described in the Material and Methods section.

atomistic description of the interaction between azobenzene derivatives and the lipids.

For all the lipids, the interaction energy was negative, confirming a favourable interaction between the azobenzene derivatives and the lipids mimicking the plasma membranes of bacteria (Fig. 5). The energy of interaction is significantly lower for *trans*-Hex-AZOTAI **4d** in presence of PE, confirming once again the specificity of this lipid for the compound.

The visualization of the molecular assemblies of each lipid with both azobenzene derivatives (Fig. 6) clearly showed a distinct positioning of *trans*-Hex-AZOTAI **4d** towards PE, compared to that seen with other lipids towards PE and that between *trans*-Bu-AZOTAI **4c** with

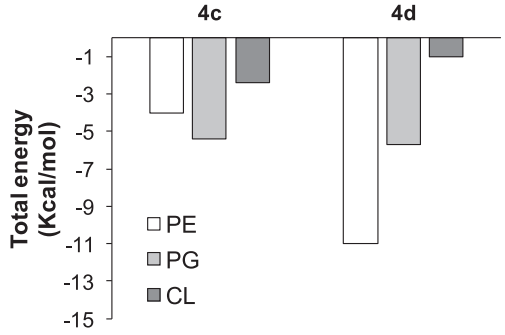

Fig. 5. Total energy of interaction of **4c** (*trans*-Bu-AZOTAI) or **4d** (*trans*-Hex-AZOTAI) with PE (phosphatidylethanolamine), PG (phosphatidylglycerol), and CL (cardiolipin) in a multimolecular monolayer assembly, calculated by Hypermatrix docking method.

all the lipids. The hydrophilic/hydrophobic repartition of **4d** perfectly matched with that of PE (Fig. 6**D**), i.e. the Azo group was facing the C=O group of PE while this is not the case for the other systems. This preferential positioning led to reduced distances between **4d** and PE as shown in Table 3.

3. General discussion

Antibacterial experiments showed that *trans*-Hex-AZOTAI **4d,** with six carbon atoms in the alkyl chain, exhibited a relatively high antibacterial activity against both gram-positive and gram-negative bacteria and that *trans*-Bu-AZOTAI **4c**, with four carbon atoms in the alkyl chain, also showed significant antibacterial activity against a gram-positive bacterium. We also showed that **4c** and **4d** can insert into a lipid membrane. This can lead to the destabilization of bacterial membrane, as observed with permeability assays. Although compounds **4c** and **4d** showed an energetically favourable interaction with all the tested lipids, interactions with PE was the most favourable**,** especially for *trans*-Hex-AZOTAI **4d**. It suggests that the inner plasma membrane of the bacteria can be the target of our compounds.

Although the calcein leakage experiments showed a clear dependence between the destabilization effect of *trans*-Hex-AZOTAI **4d** compounds and the PE content, we cannot implicate only PE as the lipid involved in the process of permeabilization of the bacterial membrane by the azobenzene molecules. Indeed, a higher MIC_{50} value of *trans*-Hex-AZOTAI **4d** compound was observed for *E. coli*, which displays the higher PE content in its plasma membrane composition compared to *B. subtilis* plasma membrane. A possible explanation for this phenomenon can be the presence of an outer membrane in the gram-negative bacteria. The latter is composed of lipopolysaccharides that could partially prevent the azobenzene molecule from reaching the inner plasma membrane and lower antibacterial activity of our compounds on the gram-negative strain compared to the gram-positive bacteria.

4. Conclusion

We synthesized four amphiphilic cationic azobenzenes differing in their alkyl chain length and evaluated their antibacterial activities against a gram-negative and a gram-positive bacterium. Among them, *trans*-Hex-AZOTAI **4d**, with six carbon atoms in the alkyl chain, displayed a high activity against the two bacterial models, whereas *trans*-Bu-AZOTAI **4c**, with four carbon atoms in the alkyl chain, displayed high activity against only the gram-positive bacterium *B. subtilis*. We investigated the membrane interaction of both molecules by experimental and *in-silico* biophysical approaches. Results suggest that the biological activity of **4c** and **4d** could be linked to their interaction with the bacterial membrane favoured by the presence of PE.

5. Experimental section

5.1. Synthesis

All commercially available products and solvents were used without further purification. Reactions were monitored by TLC (Kieselgel 60F254 aluminium sheet). Column chromatography was performed on silica gel 40–60 µm. Flash column chromatography was performed on an automatic apparatus, using silica gel cartridges. ^1H and ^{13}C NMR spectra were recorded on a 400 MHz/54 mm ultralong hold. Chemical shifts (δ) are quoted in parts per million (ppm) and are referenced to TMS as an internal standard.

5.1.1. Synthesis of a *1a–1d*

Syntheses following procedure in literature [3]. Analysis are consistent with the literature. **1a** [33] 3.31 g, 18% yield. ^1H NMR (400 MHz, $CDCl_3$): δ 7.88 (4H, m); 7.48 (3H, m); 6.95 (2H, d, J = 8.6 Hz). ^{13}C: δ 158.4; 152.8; 147.3; 130.6; 129.2; 125.2; 122.7;

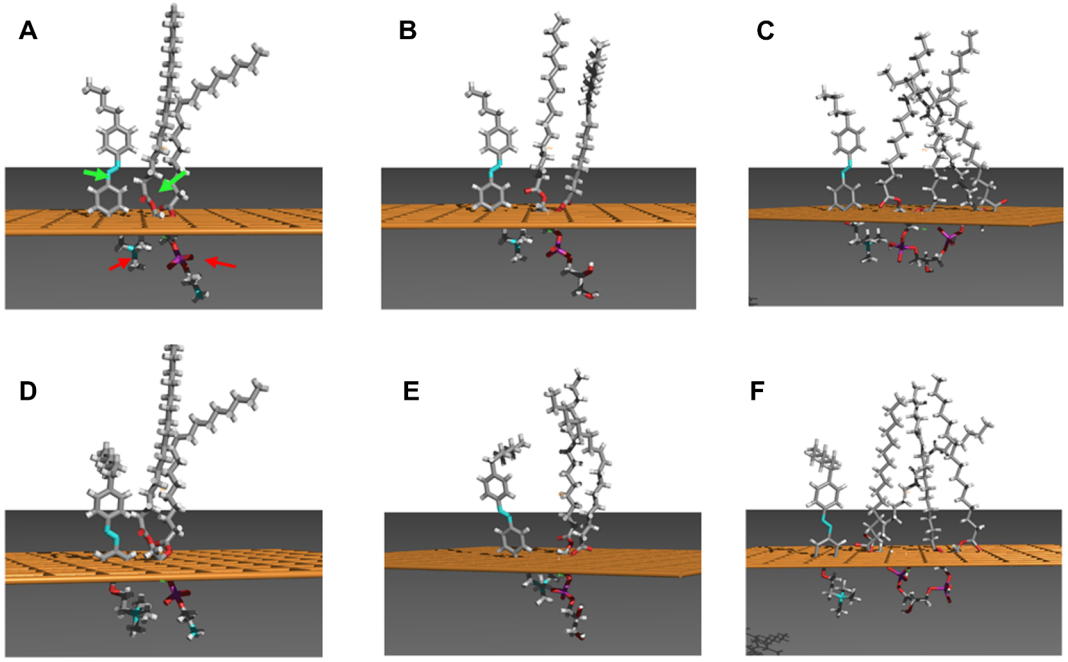

Fig. 6. Interaction between *trans*-Bu-AZOTAI **4c** (A, B, C-upper panel) or *trans*-Hex-AZOTAI **4d** (D, E, F-lower panel) and PE (phosphatidylethanolamine) (A and D), PG (phosphatidylglycerol) (B and E) and CL (cardiolipin) (C and F) calculated using the hypermatrix docking method. The orange plane represents the hydrophobic (above the plane)/hydrophilic (below the plane) interface. The green arrows in Fig. 6A point to the atoms taken as references for the N—O distance calculations and the red arrows, to the atoms taken as references for the N—P distance.

Table 3
Distance (in Å) between the N atom from the amine group of the Azo molecules and the phosphorus atom from the phospholipid considered (first column) and between the N atom from the azo group (Azo molecules) and the oxygen of the closest carbonyl group from the phospholipid considered (second column). PE: phosphatidylethanolamine, PG: phosphatidylglycerol and CL: cardiolipin.

	Distance N—P (Å)	Distance N—O (Å)
4c-PE	5.1	6.1
4d-PE	4.7	2.9
4c-PG	5.1	4.6
4d-PG	4.8	11.3
4c-CL	4.8	6.2
4d-CL	9.1	9.2

115.9 **1b** [34] 17.07 g, 75% yield. ^{1}H NMR (400 MHz, $CDCl_3$): δ 7.86 (2H, d, J = 7.4 Hz); 7.81 (2H, d, J = 8.1 Hz); 7.32 (2H, d, J = 8.1 Hz); 6.93 (2H, d, J = 8.8 Hz); 2.72 (2H, q, J = 7.6 Hz); 1.28 (3H, t, J = 7.6 Hz) ^{13}C: δ 158.3; 150.9; 147.4; 147.2; 126.7 (×2); 125 (×2); 122.8 (×2); 116 (×2); 28.9; 15.6 **1c** [35] 16.71 g, 79% yield. ^{1}H NMR (400 MHz, $CDCl_3$): δ 7.85 (2H, d, J = 8.8 Hz); 7.79 (2H, d, J = 8.3 Hz); 7.30 (2H, d, J = 8.3 Hz); 6.92 (2H, d, J = 8.8 Hz); 2.68 (2H, t, J = 7.7 Hz); 1.75 (1H, s); 1.64 (2H, q, J = 7.6 Hz); 1.37 (2H, m); 0.94 (3H, t, J = 7.3 Hz) ^{13}C: δ 158.0; 150.8; 147.1; 145.9; 129.0 (2×); 124.7 (2×); 122.5 (2×); 115.7 (2×); 35.5; 33.4; 22.3; 13.9 **1d** [18] 14.82 g, 51% yield ^{1}H NMR (400 MHz, $CDCl_3$): δ 7.86 (2H, d, J = 8.6 Hz); 7.8 (2H, d, J = 8.1 Hz); 7.3 (2H, d, J = 8.6 Hz); 6.94 (2H, m); 2.67 (2H, t, J = 7.6 Hz); 1.65 (2H, m); 1.32 (6H, m); 0.89 (3H, t, J = 7.3 Hz) ^{13}C: δ 158.3; 150.3; 147.2; 146.2; 129.2 (×2); 125 (×2); 122.7 (×2); 115.9 (×2); 36; 31.9; 31.4; 29.1; 22.7; 14.2.

5.1.2. Synthesis of a *2a–2d*

To a solution of 4-alkyl-4′-hydroxyazobenzene (**1a–1d,** 19.7 mmol) in butan-1-ol (15 mL) K_2CO_3 (2.72 g, 19.7 mmol) and KI (116 mg, 0.7 mmol) were dissolved. Then, 2-chloroethanol (2.8 mL, 39.4 mmol) was added dropwise and the mixture was refluxed for 24 h. After filtration under vacuum, the solvent was evaporated. The residue was purified by silica gel chromatography (Cyclohexane/EtOAc, 7:3) to obtain compounds **2a–2d**. **2a** [36] (orange solid, 2.21 g, 79% yield) ^{1}H NMR (400 MHz, $CDCl_3$): δ 7.91 (4H, dd, J_1 = 8.1 Hz, J_2 = 12.7 Hz); 7.48 (3H, m); 7.01 (2H, d, J = 8.9 Hz); 4.14 (m, 2H); 3.99 (m, 2H). ^{13}C: δ 161.1; 152.8; 147.3; 130.3; 129.1 (×2); 124.9 (×2); 122.7 (×2); 114.9 (×2); 69.6; 61.3. **2b** (orange solid, 3.58 g, 67% yield) mp = 126 °C, ^{1}H NMR (400 MHz, $CDCl_3$): δ 7.83 (2H, d, J = 9.2 Hz); 7.74 (2H, d, J = 8.4 Hz); 7.21 (2H, d, J = 8.4 Hz); 6.95 (2H, d, J = 8.8 Hz); 4.10 (m, 2H); 3.93 (m, 2H); 2.65 (q, 2H, J = 7.6 Hz); 1.21 (t, 2H, J = 7.6 Hz). ^{13}C: δ 160.9; 151.1; 147.5; 147.4; 128.6 (×2); 124.7 (×2); 122.8 (×2); 114.9 (×2); 69.6; 61.5; 29.0; 15.6., FTIR: 3334 cm^{-1} (w), 2931 cm^{-1} (w), 1597 cm^{-1} (s), 1500 cm^{-1} (s), 1252 cm^{-1} (s), 1079 cm^{-1} (s), 1045 cm^{-1} (s), 848 cm^{-1} (s), 841 cm^{-1} (w) HRMS (ESI+) *m/z* calculated for $[(C_{16}H_{18}N_2O_2)H]^+$ 368.2696.1227 found 368.2709 **2c** [37] (orange solid, 1.98 g, 34% yield) ^{1}H NMR (400 MHz, $CDCl_3$): δ 7.88 (2H, d, J = 9.0 Hz); 7.81 (2H, d, J = 8.4 Hz); 7.31 (2H, d, J = 8.5 Hz); 7.03 (2H, d, J = 9.0 Hz); 4.17 (2H, t, J = 4.5 Hz); 4.01 (2H, m); 2.68 (2H, t, J = 7.7 Hz); 1.64 (2H, m); 1.38 (2H, sex, J = 7.4 Hz); 0.95 (3H, t, J = 7.3 Hz) ^{13}C: δ 158.0; 150.8; 147.1; 145.9; 129.0 (×2); 124.7 (×2); 122.5 (×2); 115.7 (×2); 35.5; 33.4; 22.3; 13.9 **2d** [37] (orange solid, 2.61 g, 40% yield) ^{1}H NMR (400 MHz, $CDCl_3$): δ 7.90 (2H, d, J = 8.4 Hz); 7.80 (2H, d, J = 7.8 Hz); 7.30 (2H, d, J = 7.7 Hz); 7.03 (2H, d, J = 8.4 Hz); 4.16 (2H, m); 4.01 (2H, m); 2.67 (2H, t, J = 7.6 Hz); 1.65 (2H, m); 1.31 (6H, m); 0.89 (3H, m) ^{13}C: δ 160.9; 151.1; 147.5; 146.2; 129.2 (×); 124.7 (×2); 122.7 (×2); 114.9 (×2); 69.6; 61.5; 36.0; 31.4; 29.1; 22.7; 19.1; 14.2

5.1.3. Synthesis of a *3a–3d*

To a solution of **2a–2d** (4 mmol) dichloromethane (25 mL), trimethylamine (1 mL, 6.2 mmol) and 4-dimethylaminopyridine (15 mg, 2 mol%) were added. Tosyl chloride (1.2 g, 6.2 mmol) was added slowly to the mixture at 0 °C. The mixture was then stirred at ambient temperature for 24 h. The residue was extracted with a saturated solution of NH_4Cl (2 × 20 mL), then with a saturated solution of $NaHCO_3$ (2 × 20 mL) and then with H_2O (2 × 20 mL). These compounds were used without any purification in the next step.

5.1.4. Synthesis of a 4a–4d

Compounds **3a–3d** was dissolved in a H_2O/acetone mixture (2:1). To this, a solution of dimethylamine (1.4 mL, 8.2 mmol, 40%wt in water) was added. The mixture was refluxed for 24 h. The acetone was then evaporated, and mixture was extracted with EtOAc (3x40mL). The collected organic phase was washed with a saturated solution of K_2CO_3 (2x40mL) and by H_2O (2x40mL). The organic layer was dried with $MgSO_4$. After evaporation, the residue was dissolved in 150 mL of diethyl ether. Then, methyl iodide (1 mL, 16 mmol) was added. The mixture was stirred at ambient temperature for 24 h. The product was then filtered under vacuum.

Trans-H-AZOTAI **4a** [38] orange solid, 164 mg, 10% yield. ^{1}H NMR (400 MHz, DMSO-d_6): δ 7.95 (2H, d, J = 8.2 Hz); 7.86 (2H, d, J = 7.3 Hz); 7.58 (2H, d, J = 6.9 Hz); 7.22 (2H, d, J = 8.5 Hz); 4.59 (2H, s); 3.83 (2H, s); 3.2 (9H, s) ^{13}C: δ 160.1; 151.9; 146.6; 143.4; 129.4 (×2); 124.6 (×2); 122.3 (×2); 115.4 (×2); 64; 62.1; 53.1 (×3).

Trans-Et-AZOTAI **4b** [39] orange solid, 439 mg, 25% yield. ^{1}H NMR (400 MHz, MeOD): δ 7.92 (2H, d, J = 8.8 Hz); 7.80 (2H, d, J = 8.1 Hz); 7.36 (2H, d, J = 8.1 Hz); 7.12 (2H, d, J = 8.8 Hz); 4.6 (2H, s); 3.93 (2H, s); 3.26 (9H, s); 2.72 (2H, q, J = 7.2 Hz); 1.27 (3H, t, J = 7.6 Hz) ^{13}C: δ 161.1; 149.1; 149.0; 129.5 (×2); 125.6 (×2); 124.1 (×2); 115.8 (×2); 66.5; 63.5; 54.9 (×3); 38.4; 29.8; 16.0.

Trans-Bu-AZOTAI **4c** [40] orange solid, 1.83 g, 98% yield. ^{1}H NMR (400 MHz, MeOD): δ 7.92 (2H, d, J = 9.0 Hz); 7.79 (2H, d, J = 8.3 Hz); 7.33 (2H, d, J = 8.3 Hz); 7.18 (2H, d, J = 9.0 Hz); 4.60 (2H, s); 3.92 (2H, s); 3.31 (9H, s); 2.69 (2H, t, J = 7.7 Hz); 1.64 (2H, m); 1.39 (2H, m); 0.95 (3H, t, J = 7.4 Hz) ^{13}C: δ 161.1; 152.2; 149.0; 147.6; 130.3 (2×); 125.7 (2×); 123.7 (2×); 116.2 (2×); 66.5; 63.5; 3 × 54.9; 36.5; 34.8; 23.4; 14.3.

Trans-Hex-AZOTAI **4d** orange solid, 495 mg, 25% yield. mp = 196 °C ^{1}H NMR (400 MHz, MeOD) 7.92 (2H, d, J = 8.7 Hz); 7.79 (2H, d, J = 8.0 Hz); 7.34 (2H, d, J = 8.0 Hz); 7.18 (2H, d, J = 8.7 Hz); 4.6 (2H, s); 3.92 (2H, s); 3.31 (9H, s); 2.70 (2H, t, J = 7.6 Hz); 1.66 (2H, m); 1.34 (6H, m,); 0.90 (3H, m) ^{13}C: δ 161.1; 152.3; 149.1; 147,1; 130.2 (×2); 125.7 (×2); 123.7 (×2); 116.2 (×2); 66.5; 63.5; 49 (×3); 36.8; 32.9; 32.6; 30.0; 23.7; 14.4. FTIR: 2928 cm^{-1} (w), 1737 cm^{-1} (w), 1600 cm^{-1} (w), 1500 cm^{-1} (w), 1243 cm^{-1} (s), 1155 cm^{-1} (w), 1059 cm^{-1} (w), 953 cm^{-1} (s), 843 cm^{-1} (s) HRMS (ESI+) m/z calculated for $[(C_{46}H_{38}I_2N_6O_2)H]^+$ 863.4443.1227 found 863.4522.

5.2. Surface tension measurements at air-water interface

Adsorption at the air-water interface was analysed at room temperature with an automated Langmuir Balance system equipped with a wire probe (MicroTrough X, Kibron Helsinki, 15.9 cm^2). Compounds **4a–4d** were solubilised in DMSO and dispersed (20 µL) into the subphase (MilliQ water) to a range of final concentrations (C from 15 µg/mL to 1750 µg/mL). The subphase was stirred, during the whole experimentation. The surface pressure was recorded until its value reached the equilibrium (Πeq). CMC was determined from the plot Πeq = f (C) at the intersection between the linear regression of the ascendant and plateau parts.

5.3. In vitro antibacterial activity

5.3.1. Bacterial strains

E. coli strain ATCC 25922 and *B. subtilis* strain ATCC 6051 were used. Both bacteria were grown on solid trypticase-soy-agar medium on Petri dish. Bacteria were reserved at 4 °C and replicated at least every week.

5.3.2. Determination of minimum inhibitory concentrations (MICs)

Assays were carried out in 96-well clear flat-bottom plates in triplicates using a method based on CLSI broth microdilution method [41]. Briefly, 100 µL of bacterial suspension from a culture inoculated with a 24 h aged colony on TSA and grown overnight at 30 °C in a mineral medium (KCl 0.250 g/L, NaH_2PO_4 1.544 g/l, $Na_2HPO_4{\cdot}2H_2O$ 0.008 g/L, $MgSO_4$ 0.244 g/L, NH_4NO_3 1 g/L, $MgCl_2$ 0.05 g/L; pH = 5,) was added to each well. A 2 µL aliquot of the solution of test compound in 1–2% DMSO was added and the volume was made up to 200 µL with mineral medium. A source of glucose was added to the mineral medium to maintain a final glucose concentration of 10 g/L. Mother solutions of compounds were replaced by the DMSO based solvent without compound in controls. Bacterial growth was monitored by measuring absorbance at 600 nm every 15 min over 24 h. The growth inhibition of the bacteria in the test wells was calculated using the following equation:

$$\%_{Inhibition} = \left(1 - \frac{OD_{var\ \ test}}{OD_{var\ \ control}}\right) \times 100$$

where $OD_{var\ test}$ is the difference of optical density between the highest point and the lowest point of the growth curve of the bacterium for a test. $OD_{var\ control}$ is the difference of optical density between the highest point and the lowest point of the growth curve of the bacterium in the control without antimicrobial compound. A range of concentrations was tested for each single compound (30 µg/mL, 15 µg/mL, 7.5 µg/mL, 3.75 µg/mL, 2 µg/mL, 1 µg/mL). The weaker tested concentration triggering at least 50% of growth inhibition was defined as MIC_{50}.

5.4. Interaction to bacterial membrane models

5.4.1. Leakage experiments

The leakage of entrapped self-quenched calcein from LUVs induced by a permeabilizing agent can be monitored by the increase of fluorescence caused by its dequenching further to dilution [42]. LUVs of *E. coli*-like, *B. subtilis*-like, and Test-LUVs were prepared in a saline-Tris-HCl buffer (150 mM NaCl, 10 mM TRIS, pH 7.5) with a self-quenching concentration of calcein (10 mM). *E. coli*-like LUVs were composed of 70% of phosphatidylethanolamine (PE), 25% of phosphatidylglycerol (PG), and 5% of cardiolipin (CL). *B. subtilis*-like LUVs were composed of 14% PE, 81% PG, and 5% CL. The last type of LUVs were PE-free LUVs that were composed of 95% PG and 5% CL. For all LUVs, the un-encapsulated dye was removed on a gel column of Sephadex G75. The purified calcein-filled LUVs were put in contact with either a 0.5% solution of Triton-X as a "maximal" permeabilizing agent, with DMSO as a "minimal" permeabilizing, and with a solution of *trans*-Bu-AZOTAI **4c** and *trans*-Hex-AZOTAI **4d** *at* $C_{azobenzene}/C_{lipids}$ *molar* ratio of 0.25 dissolved in DMSO. The total concentration of lipids was between 9 µM and 16 µM. The excitation and emission wavelengths were 472 and 512 nm, respectively, and the fluorescence was measured over a period of 900 *sec*. The percentage of released calcein (% leakage) was calculated using the formula:

$$\%Leakage = \left|\frac{F_{exp} - F_{DMSO}}{F_{triton} - F_{DMSO}}\right| \times 100$$

where F_{exp} is the fluorescence signal for a given concentration of azobenzene, F_{DMSO} is the fluorescence signal for LUVs with DMSO, and F_{triton} is the fluorescence signal of LUVs incubated with 0.5% Triton X-100. The azobenzene solution concentrations used during the *in vitro* techniques were optimized so that measurements would fall between the lower limit of measurement and the limit of saturation. Two independent repetitions were performed.

5.4.2. Adsorption experiments into a lipid monolayer

Adsorption experiments were performed in a KSV Minitrough (Helsinki, Finland, 7.5 × 20 cm^2). The subphase was milliQ water (~80 mL) with a constant temperature at 22.0 ± 1.0 °C. The subphase was continuously stirred with a magnetic stirrer. Pure PE, pure PG or pure CL molecules in chloroform/methanol (2/1 v/v) solvent, was spread at the air-water interface to reach the desired initial surface pressure. After 20 min of waiting for solvent evaporation and film

stabilization, *trans*-Bu-AZOTAI **4c** or *trans*-Hex-AZOTAI **4d** in DMSO solution was injected underneath the preformed lipid monolayer. The final subphase concentration was 10 μM for both **4c** and **4d**. Their adsorption to the lipid monolayers was followed by the increase in surface pressure. As a control experiment, the same volume of pure DMSO was injected underneath the lipid monolayer, and no change in the surface pressure was observed. Maximal insertion pressure (MIP) corresponds to the surface pressure beyond which no adsorption occurs. It was obtained by linear regression of the plot ΔΠ vs Πi at the intersection with the *x* axis. The "differential Π_0 ($d\Pi_0$)" corresponds to the difference between $\Delta\Pi_0$ which is the y-intercept of the linear regression of the ΔΠ vs Πi plot, and Πe which is the surface pressure increase at the equilibrium obtained in an independent experiment performed at the same **4c** or **4d** concentration but without lipids spread at the interface.

While a positive $d\Pi_0$ indicates affinity of the compound for the tested lipid monolayer, a negative value of $d\Pi_0$ points to an unfavourable impact of lipid on the molecule insertion. The uncertainties in MIP and the $\Delta\Pi_0$ were calculated as described previously [41].

5.4.3. Simulation of azobenzene-model membrane interaction

The interactions of **4c** or **4d** with model membranes were analysed by molecular modelling. The 3D structures of **4c**, **4d**, PE, PG, and CL were constructed using HyperChem software (Hypercube, Inc.). The molecular geometry was optimized with the steepest-descent method using the MM + force field, and a systematic analysis of the torsion angles using the structure tree method was performed as described previously [43]. The most probable structure corresponding to the lowest conformational energy was used for further calculations.

The insertion of the molecule within an implicit bilayer was computed by the IMPALA procedure as described in Ducarme et al. [27] and the interaction energies in a lipid monolayer (PE, PG or CL) were calculated using the simple docking method called Hypermatrix.

Briefly, the IMPALA method is based on a Monte Carlo approach using an implicit description of membrane. The latter is modelled with an implicit membrane and described as a continuous medium whose properties vary along the axis perpendicular to the bilayer plane (z axis). The forcefield was parameterized to mimic a membrane in aqueous environment by considering (1) the hydrophobic effect between the membrane and a solute (Epho) and (2) the perturbation effect of the solute on the lipid acyl chain organization (Elip). The two restraints were calculated and summed at each position of the Azo molecule into the implicit membrane; the molecule was systematically moved along the z axis by 1 Å steps, from one side of the membrane to the other. A profile of the total energy restraint (Epho + Elip) as a function of the mass centre penetration into the implicit bilayer was then obtained.

The Hypermatrix method is described in detail elsewhere [43]. Briefly, the synthetic Azo molecule was put in a fixed position at the centre of the system and oriented at the hydrophobic/ hydrophilic interface, while the lipid molecule, also oriented at the lipid/water interface, was positioned around the molecule by rotations and translations (more than 10 million positions were tested). For each position, an energy value was calculated, according to a home-designed force field [43]. The energy values together with the coordinates of all assemblies were stored in a matrix and classified, according to decreasing values. The first stable match was considered as the best assembly between the two molecules.

Declarations of Competing Interest

The authors declare to have no competing interest.

Acknowledgements

This work was financed by 'Wallonie-Bruxelles International', 'Fonds National de la Recherche Scientifique pour la communauté française de Belgique', 'Ministère des Affaires Etrangères et du Développement International (MAEDI)', 'Ambassade de France en Belgique pour la France', A.F thanks the 'Ministère de l'Education Nationale de la Recherche et de la Technologie' for his research fellowship.M.D. and L.L. thank the F.R.S.-F.N.R.S. for their position as Senior Research Associate.

Appendix A. Supplementary material

Supplementary data to this article can be found online at https://doi.org/10.1016/j.bioorg.2019.103399.

References

[1] WHO publishes list of bacteria for which new antibiotics are urgently needed http://www.who.int/news-room/detail/27-02-2017-who-publishes-list-of-bacteria-for-which-new-antibiotics-are-urgently-needed (accessed Oct 23, 2018).
[2] V. Defraine, M. Fauvart, J. Michiels, Fighting bacterial persistence: current and emerging anti-persister strategies and therapeutics, Drug Resist. Updat. 38 (2018) 12–26, https://doi.org/10.1016/j.drup.2018.03.002.
[3] N. Drillaud, E. Banaszak-Léonard, I. Pezron, C. Len, Synthesis and evaluation of a photochromic surfactant for organic reactions in aqueous media, J. Org. Chem. 77 (21) (2012) 9553–9561, https://doi.org/10.1021/jo301466w.
[4] M. Billamboz, F. Mangin, N. Drillaud, C. Chevrin-Villette, E. Banaszak-Léonard, C. Len, Micellar catalysis using a photochromic surfactant: application to the Pd-catalyzed Tsuji-Trost reaction in water, J. Org. Chem. 79 (2) (2014) 493–500, https://doi.org/10.1021/jo401737t.
[5] T.J. Sorensen, K. Kjaer, D.W. Breiby, B.W. Laursen, Synthesis of novel amphiphilic azobenzenes and X-ray scattering studies of their langmuir monolayers, Langmuir 24 (2008) 3223–3227.
[6] E. Léonard, F. Mangin, C. Villette, M. Billamboz, C. Len, Azobenzenes and catalysis, Catal. Sci. Technol. 6 (2) (2016) 379–398, https://doi.org/10.1039/C4CY01597E.
[7] R. Rajaganesh, A. Gopal, T. Mohan Das, A. Ajayaghosh, Synthesis and properties of amphiphilic photoresponsive gelators for aromatic solvents, Org. Lett. 14 (3) (2012) 748–751, https://doi.org/10.1021/ol203294v.
[8] G. Galli, E. Chiellini, Azobenzene containing polymers: what is yet viable with aged liquid crystals, Liq. Cryst. 33 (2006) 1297–1301.
[9] S.S. Subala, B.S. Sundar, S.S. Sastry, Synthesis and characterization of nonsymmetric liquid crystal dimer containing biphenyl and azobenzene moiety, J. Chem. 2013 (2013) e939406, https://doi.org/10.1155/2013/939406.
[10] J. Salta, R.I. Benhamou, I.M. Herzog, M. Fridman, Tuning the effects of bacterial membrane permeability through photo-isomerization of antimicrobial cationic amphiphiles, Chem. – Eur. J. 23 (52) (2017) 12724–12728, https://doi.org/10.1002/chem.201703010.
[11] S.M. Tawfik, H.H. Hefni, Synthesis and antimicrobial activity of polysaccharide alginate derived cationic surfactant–metal(II) complexes, Int. J. Biol. Macromol. 82 (2016) 562–572, https://doi.org/10.1016/j.ijbiomac.2015.09.043.
[12] J.G. Lundin, P.N. Coneski, P.A. Fulmer, J.H. Wynne, Relationship between surface concentration of amphiphilic quaternary ammonium biocides in electrospun polymer fibers and biocidal activity, React. Funct. Polym. 77 (2014) 39–46, https://doi.org/10.1016/j.reactfunctpolym.2014.02.004 (Copyright (C) 2019 American Chemical Society (ACS). All Rights Reserved.).
[13] R. Kügler, O. Bouloussa, F. Rondelez, Evidence of a charge-density threshold for optimum efficiency of biocidal cationic surfaces, Microbiology 151 (5) (2005) 1341–1348.
[14] A.A. Neyfakh, V.E. Bidnenko, L.B. Chen, Efflux-mediated multidrug resistance in bacillus subtilis: similarities and dissimilarities with the mammalian system, Proc. Natl. Acad. Sci. U. S. A. 88 (11) (1991) 4781–4785.
[15] F. Alhashash, V. Weston, M. Diggle, A. McNally, Multidrug-resistant escherichia coli bacteremia, Emerg. Infect. Dis. 19 (10) (2013), https://doi.org/10.3201/eid1910.130309.
[16] J. Pérez-Miqueo, A. Altube, E. García-Lecina, A. Tron, N.D. McClenaghan, Z. Freixa, Photoswitchable azobenzene-appended iridium(Iii) complexes, Dalton Trans. 45 (35) (2016) 13726–13741, https://doi.org/10.1039/C6DT01817C.
[17] K.-Z. Fan, M. Bradley, B. Vincent, C.F.J. Faul, Effect of chain length on the interaction between modified organic salts containing hydrocarbon chains and poly(N-isopropylacrylamide-co-acrylic acid) microgel particles, Langmuir 27 (2011) 4362–4370, https://doi.org/10.1021/la104411j (Copyright (C) 2019 American Chemical Society (ACS). All Rights Reserved.).
[18] C. Blayo, J.E. Houston, S.M. King, R.C. Evans, Unlocking structure-self-assembly relationships in cationic azobenzene photosurfactants, Langmuir 34 (2018) 10123–10134, https://doi.org/10.1021/acs.langmuir.8b02109 (Copyright (C) 2019 American Chemical Society (ACS). All Rights Reserved.).
[19] N.K. Sharma, M. Singh, A. Bhattarai, Hydrophobic study of increasing alkyl chain length of platinum surfactant complexes: synthesis, characterization, micellization, thermodynamics, thermogravimetrics and surface morphology, RSC Adv. 6 (93) (2016) 90607–90623, https://doi.org/10.1039/C6RA20330B.
[20] J. Oremusová, Micellization of alkyl trimethyl ammonium bromides in aqueous solutions-Part 1: Critical micelle concentration (CMC) and ionization degree, Tenside Surfactants Deterg. 49 (3) (2012) 231–240, https://doi.org/10.3139/113.110187.
[21] A. Petek, M. Krajnc, A. Petek, The role of intermolecular interactions in the micellization process of alkyltrimethyl ammonium bromides in water, Tenside

Surfactants Deterg. 53 (1) (2016) 56–63, https://doi.org/10.3139/113.110410.
[22] L. Poirel, A. Jayol, P. Nordmann, Polymyxins: antibacterial activity, susceptibility testing, and resistance mechanisms encoded by plasmids or chromosomes, Clin. Microbiol. Rev. 30 (2) (2017) 557–596, https://doi.org/10.1128/CMR.00064-16.
[23] J.A. Silverman, N.G. Perlmutter, H.M. Shapiro, Correlation of daptomycin bactericidal activity and membrane depolarization in staphylococcus aureus, Antimicrob. Agents Chemother. 47 (8) (2003) 2538–2544, https://doi.org/10.1128/AAC.47.8.2538-2544.2003.
[24] L. Guo, M. Long, Y. Huang, G. Wu, W. Deng, X. Yang, B. Li, Y. Meng, L. Cheng, L. Fan, et al., Antimicrobial and disinfectant resistance of *Escherichia coli* isolated from giant pandas, J. Appl. Microbiol. 119 (1) (2015) 55–64, https://doi.org/10.1111/jam.12820.
[25] A. Buxbaum, Antimicrobial and toxicological profile of the new biocide akacid plus (R), J. Antimicrob. Chemother. 58 (1) (2006) 193–197, https://doi.org/10.1093/jac/dkl206.
[26] J. Nashida, N. Nishi, Y. Takahashi, C. Hayashi, M. Igarashi, D. Takahashi, K. Toshima, Systematic and stereoselective total synthesis of mannosylerythritol lipids and evaluation of their antibacterial activity, J. Org. Chem. 83 (13) (2018) 7281–7289, https://doi.org/10.1021/acs.joc.8b00032.
[27] Ph. Ducarme, M. Rahman, R. Brasseur, IMPALA: a simple restraint field to simulate the biological membrane in molecular structure studies, Proteins Struct. Funct. Genet. 30 (4) (1998) 357–371, https://doi.org/10.1002/(SICI)1097-0134(19980301)30:4<357::AID-PROT3>3.0.CO;2-G.
[28] R.M. Epand, R.F. Epand, Lipid domains in bacterial membranes and the action of antimicrobial agents, Biochim. Biophys. Acta BBA – Biomembr. 1788 (1) (2009) 289–294, https://doi.org/10.1016/j.bbamem.2008.08.023.
[29] R.F. Epand, P.B. Savage, R.M. Epand, Bacterial lipid composition and the antimicrobial efficacy of cationic steroid compounds (ceragenins), Biochim. Biophys. Acta BBA – Biomembr. 1768 (10) (2007) 2500–2509, https://doi.org/10.1016/j.bbamem.2007.05.023.
[30] H. Heerklotz, J. Seelig, Leakage and lysis of lipid membranes induced by the lipopeptide surfactin, Eur. Biophys. J. 36 (4–5) (2007) 305–314, https://doi.org/10.1007/s00249-006-0091-5.
[31] M. Deleu, S. Gatard, E. Payen, L. Lins, K. Nott, C. Flore, R. Thomas, M. Paquot, S. Bouquillon, D-Xylose-based bolaamphiphiles: synthesis and influence of the spacer nature on their interfacial and membrane properties, Comptes Rendus Chim. 15 (1) (2012) 68–74, https://doi.org/10.1016/j.crci.2011.10.006.
[32] D. Marsh, Lateral pressure in membranes, Biochim. Biophys. Acta BBA – Rev. Biomembr. 1286 (3) (1996) 183–223, https://doi.org/10.1016/S0304-4157(96)00009-3.
[33] C.-Y. Chen, K.-H. Li, Y.-H. Chu, Reaction-based detection of chemical warfare agent mimics with affinity ionic liquids, Anal. Chem. Wash. DC U. S. 90 (2018) 8320–8325, https://doi.org/10.1021/acs.analchem.8b01763 (Copyright (C) 2019 American Chemical Society (ACS). All Rights Reserved.).
[34] L. Johnson, B. Ringstrand, P. Kaszynski, A convenient preparation of long chain 4-(4-*n*-alkylphenylazo)phenols and their 4-pentylbenzoate esters, Liq. Cryst. 36 (2) (2009) 179–185, https://doi.org/10.1080/02678290902759210.
[35] K. Jia, X. Zhang, L. Zhang, L. Yu, Y. Wu, L. Li, Y. Mai, B. Liao, Photoinduced reconfiguration of complex emulsions using a photoresponsive surfactant, Langmuir 34 (38) (2018) 11544–11552, https://doi.org/10.1021/acs.langmuir.8b02456.
[36] C. Xiong, M. Xie, R. Sun, Responsiveness and morphology study of dual stimuli-controlled supramolecular polymer, Macromol. Rapid Commun. 38 (19) (2017) 1700358–1700366, https://doi.org/10.1002/marc.201700358.
[37] N. Yoshino, A. Nagasaki, Y. Kondo, M. Abe, Syntheses of amphiphiles containing two azobenzene units in a molecule, J. Jpn. Oil Chem. Soc. 44 (12) (1995) 1075–1085, https://doi.org/10.5650/jos1956.44.1075.
[38] A. Damijonaitis, J. Broichhagen, T. Urushima, K. Hüll, J. Nagpal, L. Laprell, M. Schönberger, D.H. Woodmansee, A. Rafiq, M.P. Sumser, et al., AzoCholine enables optical control of alpha 7 nicotinic acetylcholine receptors in neural networks, ACS Chem. Neurosci. 6 (5) (2015) 701–707, https://doi.org/10.1021/acschemneuro.5b00030.
[39] S. Pané, E. Gómez, E. Vallés, Influence of a magnetic field during the CoNi electrodeposition in the presence of magnetic nanoparticles, J. Electroanal. Chem. 615 (2) (2008) 117–123, https://doi.org/10.1016/j.jelechem.2007.12.002.
[40] S. Pané, E. Gómez, J. Garcia-Amorós, D. Velasco, E. Vallés, Modulation of the magnetic properties of CoNi coatings by electrodeposition in the presence of a redox cationic surfactant, Appl. Surf. Sci. 253 (5) (2006) 2964–2968, https://doi.org/10.1016/j.apsusc.2006.06.040.
[41] M. Deleu, E. Deboever, M.N. Nasir, J.-M. Crowet, M. Dauchez, M. Ongena, H. Jijakli, M.-L. Fauconnier, L. Lins, Linoleic and linolenic acid hydroperoxides interact differentially with biomimetic plant membranes in a lipid specific manner, Colloids Surf. B Biointerfaces 175 (2019) 384–391, https://doi.org/10.1016/j.colsurfb.2018.12.014.
[42] J. Weinstein, S. Yoshikami, P. Henkart, R. Blumenthal, W. Hagins, Liposome-cell interaction: transfer and intracellular release of a trapped fluorescent marker, Science 195 (4277) (1977) 489, https://doi.org/10.1126/science.835007.
[43] L. Lins, R. Brasseur, W.J. Malaisse, Conformational analysis of non-sulfonylurea hypoglycemic agents of the meglitinide family, Biochem. Pharmacol. 50 (11) (1995) 1879–1884, https://doi.org/10.1016/S0006-2952(99)80003-3.